MRS 2001
San Francisco
eingel. Vortrag

Molecular dynamics simulations of wafer bonding

Kurt Scheerschmidt

Max Planck Institute of Microstructure Physics, Weinberg 2,
D-06120 Halle/Saale, Germany, schee@mpi-halle.de
Tel: +49-345-5582910, Fax: +49-345-5582917

ABSTRACT

Molecular dynamics simulations using empirical potentials have been employed to describe atomic interactions at interfaces created by the macroscopic wafer bonding process. Investigating perfect or distorted surfaces of different semiconductor materials as well as of silica enables one to study the elementary processes and the resulting defects at the interfaces, and to characterize the ability of the potentials used. Twist rotation due to misalignment and bonding over steps influence strongly the bondability of larger areas. Empirical potentials developed by the bond order tight-binding approximation include π-bonds and yield enhanced interface structures, energies, and transferability to new materials systems.

INTRODUCTION

Wafer bonding, i.e. the creation of interfaces by joining two wafer surfaces, has become an attractive method for many practical applications to microelectronics, micromechanics or optoelectronics [1,2]. The macroscopic properties of bonded materials are mainly determined by the atomic processes at the interfaces during the transition from the adhesion state to the chemical bonding. Thus, the description of the atomic processes is of increasing interest to support the experimental investigations or to predict the bonding behaviour. While, in principle, it is now possible to predict material properties by using quantum-theoretical ab initio calculations with a miminum of free parameters, the only method to simulate atomic processes with macroscopic relevance is the molecular dynamics (MD) method using suitably fitted many-body empirical potentials. Such simulations enable a sufficiently large number of particles and relaxation times up to μs to be considered. However, the electronic structure and the nature of the covalent bonds can only be described indirectly. Therefore, it is of importance to find physically motivated semiempirical potentials starting mostly with the moments of the electron density and using tight-binding representations [3-5].

The MD simulations have successfully been used to describe ultra-high-vacuum bonding experiments for Si(100) [6], hydrogen passivated hydrophobic bonding processes [7], and to analyze the defect structure at bonded interfaces [8-10]. Simulations for SiC [11] were possible using the Tersoff [12] potential, whereas the predictions of the bondability of diamond have been performed using a bond-order potential [13]. Simulations of the bonding of amorphous silica (a-SiO_2) surfaces [14,15] may be the basis or a first step to describe hydrophilic wafer bonding. Conventional transmission (TEM) and high resolution electron microscopy (HREM) structure

imaging has been applied to investigate the resulting interfaces and the defect structures at an atomic level [16], the MD relaxed structures are the basis to calculate TEM and HREM images from it, which in combination with calculated IR-spectra provides a good experimental evidence of the results.

METHOD

The method of molecular dynamics (MD) solves Newton's equations of motion for a molecular system, which results in trajectories for all particles considered in the system. The calculations are performed with a fifth-order predictor-corrector algorithm using a constant volume (NVE ensemble) or a constant pressure (NpT ensemble) and time steps of the order of 0.25 fs to ensure the proper calculation of surface modes. NVE is preferred for free surfaces and simulations to calculate diffusion processes, whereas NpT enables the relaxation of the cell dimensions and the application of an outer pressure, which is important for, e.g., the glass generation and the simulation of wafer interfaces. For controlling the system temperature the velocities are slightly rescaled at each time step of solely the atoms in the outer layers of the structure model, still applying periodic boundary conditions parallel to the interfaces, which describes an energy flux or dissipation into a macroscopic embedding substrate. In addition, for straight defects created at the interfaces the system is coupled elastically to the bulk wafers.

Simple pair potentials and potentials of the valence force field or related types are restricted in their validity to solely small deviations from the equilibrium. A better potential most often used for semiconductors is the Stillinger-Weber (SW) potential, consisting of 2- and 3-body interactions [17]. It allows the next neighbour interaction to be included by rescaling, which is a presupposition to the simulation of the dynamical behaviour without preordered surfaces and prescribed topology. Thus, e.g., the interaction of two silicon surfaces can be studied by correctly revealing the 2x1 reconstruction of a clean Si(100) surface. The potential used for silica is the modified Born-Mayer-Huggins (BMH) ionic pair interaction combined with a weak three-body term [18]. The BMH interaction combines a repulsion and a Coulomb term, which is screened to avoid the long-range Ewald sums, the three-body term is similar to SW. In addition, a Rahman-Stillinger-Lemberg (RSL) term was used for the water interactions.

Tersoff: empirical bond order potential

The potential of Tersoff [12] with different parametrizations TI-TIII has the shape of a bond order, which is a completely different functionality than SW, BMH etc:

$$V \sim \sum [\exp(-\lambda r_{ij}) - \mathbf{b_{ij}} \exp(-\mu r_{ij})]. \qquad (1)$$

The bonds are weighted by the bond order $\mathbf{b_{ij}}$ including all many body interactions over neighbours k different from the actual bonding pair i,j, and with all parameters fitted. It predicts the asymmetric reconstruction with fourfold coordinated atoms at Si interfaces with defects. Therefore it was applied to investigate the cores of 60° partial dislocations in Si and other defects left after bonding two wafers. Parametrizations exist also to describe the silicon-hydrogen interaction, hydrocarbons, SiC, Ge, etc. (see, e.g. [19]), thus hydrogenated Si(001) surfaces are well described including reconstructions of the (1x1) and (3x1) types [7] as well as Si-SiC interactions [11]. Because of the short range of the Tersoff potential it was supposed that the bond topology is given by the usual process starting with separated Si blocks of a suitable

surface structure and orientation (surface reconstruction, steps) and applying long-range potentials initially.

Most of the existing potentials available are of the SW or T type. Compared to each other [20] they offer advantages and disadvantages in range of validity, physical meaning, fitting and accuracy as well as applicability. Such restrictions exist for other potential types, too, even if the (modified) embedded atom approximation is used (MEAM, [21]) or special environment dependencies are constructed to enhance the elastic properties near defects, as, e.g., in [22]. The interatomic forces in covalent solids, however, can only be completely described if the influence of the local environment according to the electronic structure is also included. A first step towards including such effects into an empirical description is the following bond order potential (BOP) approximation. In addition, no potential is applicable for long range interactions [23] which needs special consideration. The difficulty of developing suitable empirical potentials is threefold: One has to guess a functional form, motivated by physical intuition, fitted to ab initio and experimental data bases as well as reflecting nonfitted properties.

BOP: bond order approximation justified by TB methods

Tight binding approximations allow to develop physically motivated potentials, starting from analysis of the band energy:

$$E_{tot} = E_{rep} + E_{prom} + E_{band}(k) \qquad (2)$$

$$\text{empirical} \quad s^2p^2\text{->}sp^3 \quad \sum U_{BO}\Theta_{BO} \approx \mathbf{b_{ij}} = \pi_{ij} + (\sigma\pi_{ij} + \sigma\pi_{ji})/2 \qquad (3)$$

bond integrals — Slater-Koster [24]: ssσ, spσ, ppπ...

BOmatrix — Pettifor [5,25]: Realspace GreenFkt, Continued fraction

BOP2=>Tersoff

BOP4=> π–bonds

The repulsive energy is assumed to be an embedded pair interaction, the promotion energy reflects the energy difference of valence s and p electrons, and the band energy yields the bond order term (cf. Eq. 3). The most important part is the expansion of the bond energy into hopping matrix elements, which are given directly by the two centre integrals of Slater and Koster [24], and bond order terms. The bond order terms $\mathbf{b_{ij}}$ can be approximated by Lanczo's recursion algorithm [25], where the level of the continued fraction determines the functional form and the applicability. A second moment approximation of the tight-binding model can be used to establish a general form at the level of the Tersoff potential with at least only four free fit parameters [4]. A further enhancement is possibly based on the bond order potential (BOP4) [5], which is given up to the fourth-level continued fraction of the Greens function. Its ability is demonstrated in the application to diamond wafer bonding [13].

RESULTS

The molecular dynamics simulation starting with two perfect and parallel-oriented Si blocks with perfectly aligned 2x1 reconstructed (100) surfaces and applying a slow heat transfer approach yields perfectly bonded structures [6,7]. However, a fast heat transfer, a starting configuration, with the dimer rows in orthogonal domain orientation, or including steps or small rotational misorientations, result in configurations no longer perfectly coordinated. The energy flux at surfaces is the driving force for the bonding process. The upper terraces behave like perfect surfaces, i.e., a weak attraction owing to the next neighbour interaction initiates the dimers to rearrange and to create new bonds. The energy the bonds have gained dissipates increasing the kinetic and elastic energies of the bulk. The resulting avalanche effect implies the bonding of the lower terraces, too. However, after bonding over double layer steps a disturbed interface and defects are left which may finally relax to 60° partial dislocations or shuffle-set dislocations accompanied by a row of vacancies [8-10]. Monolayer steps rotate the dimerization direction in the neighbouring domains and give rise to a stacking fault of either intrinsic or extrinsic type, depending on the dimer orientation in the adjacent terraces. Thus the interfaces between, or outside, the single-layer steps are characterized by a 90° twist-rotation, either with metastable fivefold coordination and Pmm(m) symmetry (SW potential or fast heat transfer) or (2x2) reconstructed and P(4)m2 symmetry (TSIII). The resulting local 42m dreidl configuration has been confirmed by DFT calculations and fits two rotated half crystals of minimal structural disorder and fourfold coordination, the interface energy is reduced by approximately 20%.

Twist rotation

The effect of a small twist angle as a rotational misorientation results in a mosaic-like interface structure. Figure 1 shows such interface defect structures after the MD simulation of rotationally misoriented bonding of (100) Si wafers and, for comparison, plan view TEM images of screw dislocation networks obtained in UHV bonding experiments of similar situations (Figures 1c,d). In Figure 1a) the waferbonding itself is simulated starting with two separated Si blocks having dimerized (100) surfaces and using the SW potential in MD. After bonding and sufficient relaxation under slow heat transfer conditions, almost all atoms have a bulk-like environment separated by misfit dislocations, which may have a high rate of kinks. In Figure 1b) the MD relaxation with a TIII potential is applied to a starting model with a prescribed network of two sets of a/2[110] screw dislocations accommodating a small rotational twist. The relaxed configuration shows symmetry breaking by twice the period of the array distance corresponding to the twist angle and having two different nodes T/S1 and T/S2. They are formed by symmetrical characteristic groups of atoms having the same point group symmetry 222 (D_2) as the core structures of individual screws. Most of the atoms forming T/S1 remain fourfold with large bond-angle and bond-length distortions, but there are two atoms in the unit with a fivefold surrounding. The T/S2-nodes are formed by more complicated atomic groups, however, showing solely a fourfold coordination. In Figure 1e) simulated plan view TEM contrasts based on these structures are shown assuming different thicknesses t and beam orientations [hkl] relative to the zone axis [001]. The orthogonal networks of the experiments (cf. Figs. 1c,d) possess a regular structure over large areas, distorted by steps due to the miscut of the wafers, holes, inclusions, or amorphized regions. Depending on the twist misorientation between the bonded wafers (usually 0.1^{o} up to 3^{o}), the annealing process after the bonding, and the imaging conditions (tilt,

thickness) different details occur, which partially can be matched by the simulated images. MD simulations as well as TEM and HREM investigations showed that the screw dislocations forming the network of the (001) low-angle twist grain boundary can dissociate intrinsically into two 30° partials moving towards the bulk.

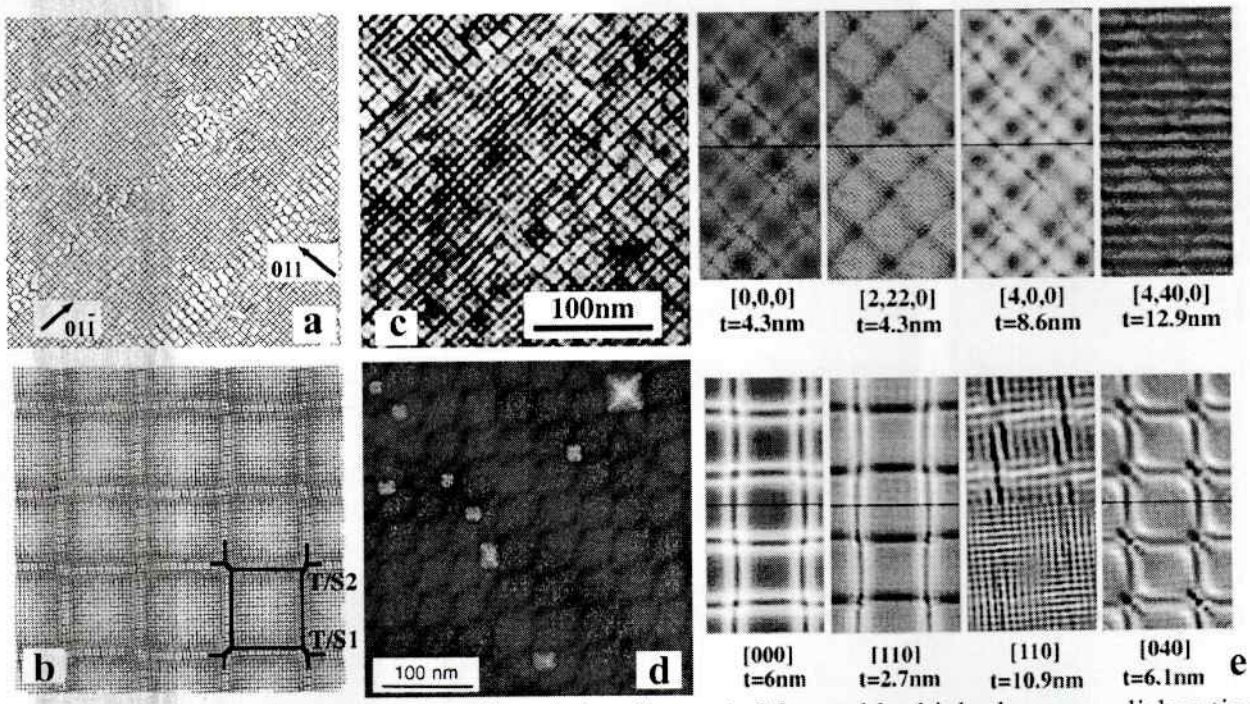

Figure 1. Rotationally misoriented waferbonding: a) Metastable kinked screw dislocation network of 4.6° rotated wafers after 2.5ps SW-MD relaxation at 900K, b) D=10b screw lattice (b=a/2<110>) at the TIII energy minimum showing two different nodes T/S1, T/S2, c,d) Experimental plan view images of screw dislocation networks of UHV-bonded (100) Si interfaces with different sample thicknesses and orientations (courtesy R. Scholz, MPI Halle), e) Simulated plan view TEM images for different thicknesses t and beam orientations indicated by the [hkl]-pole excitation (upper/lower row correspond to model a/b, resp.).

Using the Tersoff or BOP-like potentials and metastable or well-prepared starting configurations, yields further structure relaxation and energy minimization. Figure 2 shows some of the resulting minimum structures gained for higher annealing temperatures and different twist rotation angles (see Figure caption). A typical energy vs. time relaxation behaviour is shown in Figure 2a), at every temperature step - up and down - (selected are 4 of about 20 temperature steps) the system is relaxed for 25ps. Independently from the chosen twist angles and box dimensions all final structures yield finally bond energies of approximately 4.5 eV/atom at 0K. The energy gain, however, is directly related to the twist angle: approximately 0.02 eV, 0.03 eV, 0.05 eV, and 0.04 eV for 12.7°, 6.7°, 4.6°, and 2.8°, resp. The values are slightly modified if additionally steps or holes are included at the surfaces before bonding simulation starts. The maximum of energy gain between 4° and 6° twist is related to a change of the bonding behaviour itself: Whereas all simulations shown in Figure 2 with parallel dimerization at start clearly demonstrate the creation of the screw dislocation network, for orthogonal dimerization or small twist angles this is no longer valid.. As higher the annealing temperature as better the screw

formation, i.e., similar to the prescribed perfect network and its node structure, cf. Figures 1b) and 2c,d). However, the detailed investigation of the energy gain and the influence of steps as shown in Figure 2e) in relation with simulated TEM and HREM and experiments as in [26] will be done in a forthcoming paper.

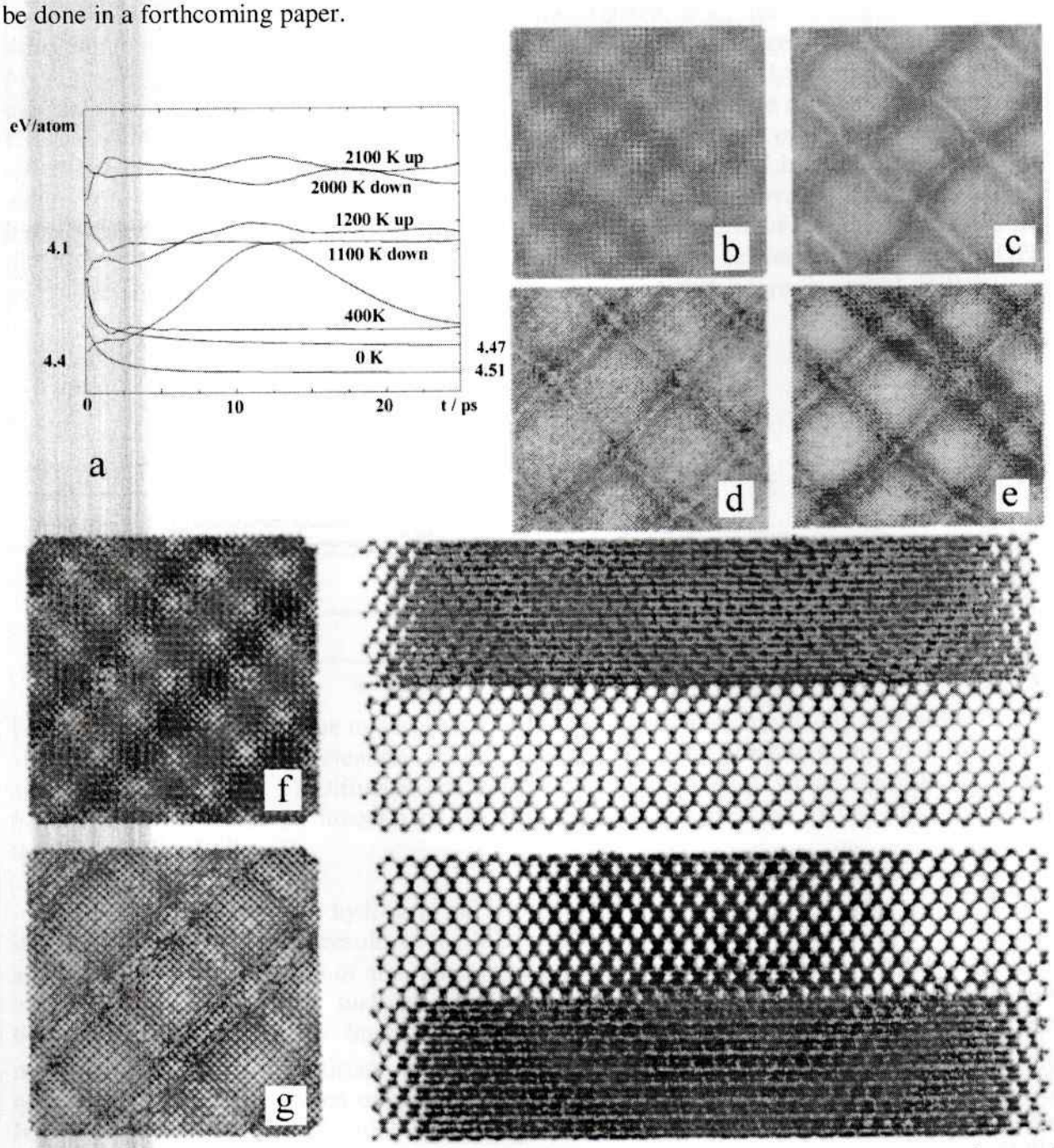

Figure 2. MD simulations of bonding rotationally twisted wafers with different angles and annealing temperatures: a) Typical energy relaxation during MD annealing cycles (up and down, three temperatures shown) starting and finnishing at 0K with -4.41 and –4.51 eV/atom, resp., b) Twist angle 2.8°, 134500 atoms, 22nm box, 2100K , orthogonal dimers, c) as b) parallel dimers, d) Twist angle 4.6°, 4.3nm box, 600K, e) as d) with [110]-steps, f) Twist angle 6.7°, 9.2nm box, 2100K , orthogonal dimers, [001] and [110] views, g) as f) with parallel dimers.

Adsorbates: H on Si and H_2O on Silica

The influence of adsorbates has been investigated, e.g., for hydrogenated surfaces assuming two Si(001)-3x1 blocks, corresponding to a hydrogen coverage of 4/3 monolayers, and NVE at 300K. A time step of 0.12 fs is used to account for the fast dynamics of the hydrogen atoms. External forces in the direction perpendicular to the interface are added to the interatomic forces of the two outermost atomic layers of each slab. The main result of the corresponding MD simulations consists in the finding of an energy barrier characterized by a critical pressure of about 80MPa to overcome the repulsion forces and to create covalent bonds across the hydrogenated interfaces. Figure 3a shows the oscillatory behaviour of the relative wafer distances below 80MPa, indicating the barrier, the bonding region between 100MPa and 1.4GPa, and the region of creating surface defects for pressures higher than approximately 1.4GPa.

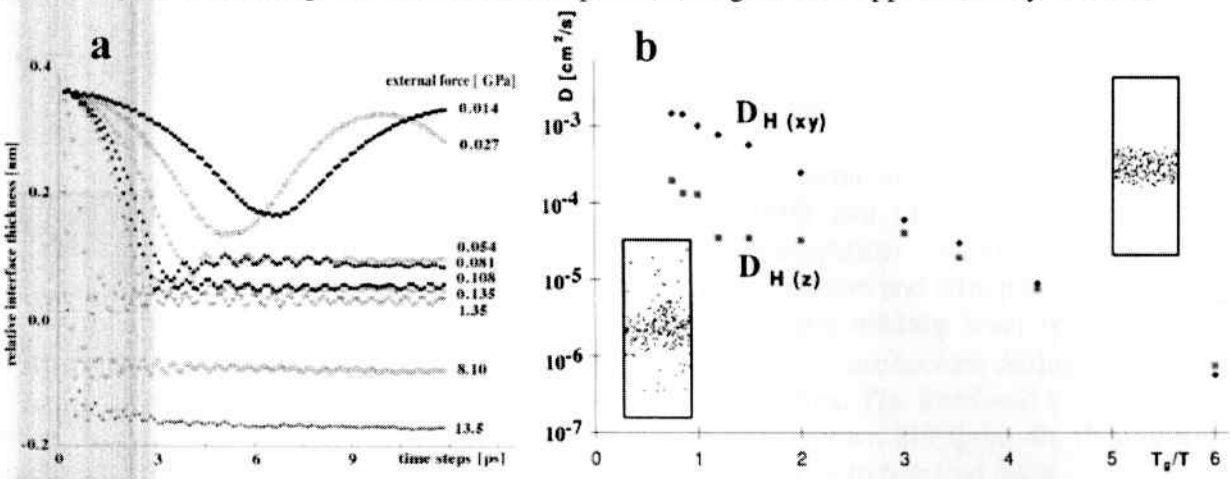

Figure 3. Energy barriers due to adsorbates: a) Transition between oscillatory behaviour (below 100MPa) and surface defect creation (above 1.4GPa) of Si wafer bonding with a hydrogen layer and applying pressure, b) Diffusion coefficients of hydrogen D_{Hxy} within and D_{Hz} across a bonded silica interface as function of the bond temparature relative to the glass transition temperature T_g of silica.

Figure 3b shows the hydrogen diffusion coefficients D_{Hxy} within and D_{Hz} across the interface as one of the main results of the MD simulation of silica amorphization, hydroxylation and bonding. The generation of amorphous silica models starts from crystalline silica structures by annealing cycles. Free surfaces were generated and the reconstructed surfaces were bombarded with H_2O groups. Such relaxed silica glasses have a highly reactive surface. Water molecules settling on the surface have at least three different kinds of bonding sites. They correlate to sites with reduced oxygen bridges, or where silanols are created by cracking Si-O bonds in the surface. Two adjoining hydroxylated surfaces, each covered with 1 to 2 monolayers of water are brought into contact to simulate the wafer bonding between silica and/or hydrophilic Si. Three different regimes are obtained, which can be related to experimental observations and the hydrogen diffusivity shown in Figure 2: The short-time behaviour at low temperatures and pressures leads to hydrogen-bonded surfaces with a low bonding energy; hydrogen has a high mobility in the gap. The bonding energy can be increased either by increasing the temperature and/or the pressure, or by tempering at lower temperatures for sufficiently long times. Increasing

the temperature and/or pressure enables to dissolve the silanol and water groups and to lower the diffusion barrier, which occurs for temperatures between $T_g/3$ and T_g, with reduced hydrogen mobility across the gap. For higher temperatures the interface gap can be closed by forming direct silica-silica bonds, resulting in equivalent diffusivity parallel and normal to the interface. The long-time behaviour shows a reactive rearrangement of the surface, which locally leads to strong silica bonds even at low temperatures.

Diamond and SiC

The Tersoff potential is well suited to describe the SiC(0001)-3x3 and $\sqrt{3}x\sqrt{3}R30^\circ$ surface reconstructions. A comparison with TB and DFT results shows that even the bond length and energy differences of the different reconstructions are correctly revealed. Applying similar simulations to the SiC(0001) wafer bonding yields for different starting configurations bond energies between 0.5 and 3.2 J/m^2. Figure 4a shows the relaxed final state for the $\sqrt{3}x\sqrt{3}R30^\circ$ initial configuration resulting in a peak-to-peak arrangement. This configuration is the energetically optimized structure for which the prediction can be made that bonding in an ultrahigh vacuum environment should be possible.

Finally, in Figure 4b the BOP4 potential is used to simulate the bonding process of diamond. Two different surfaces are considered, viz. (001) and (111) with an equivalent reconstruction. Both the tight-binding MD and the semiempirical method using a BOP4 potential, which enables one to use far more atoms in the calculation and which demonstrates the quality of the fit, show the same bonding behaviour. The tight-binding level is necessary to describe correctly the π - bonds. The dimers remain, the π - bonds are broken during the bonding process, however, there is no graphitization at lower temperatures. The fourfould coordination is the resulting stable minimum structure. On the (111) surface, shown in Figure 4b, therefore the outermost dimers must be rearranged from threefold coordinations to fourfold ones.

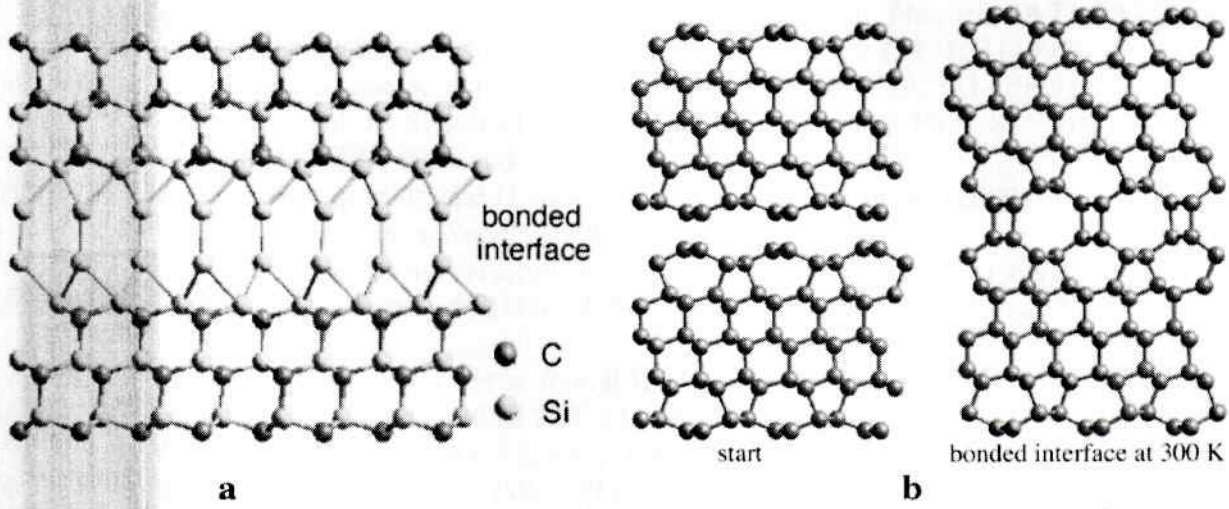

Figure 4. MD simulations of bonding SiC and diamond surfaces: a) SiC (0001)- $\sqrt{3}x\sqrt{3}R30^\circ$ in peak-to-peak arrangement, b) C (111)-2x1 and using a BOP4 potential.

CONCLUSIONS

Molecular dynamics simulations (MD) based on empirical potentials are used to investigate the elementary steps of bonding two Si(001) wafers. The system is coupled elastically to the bulk wafers, and the energy dissipation is controlled by the transfer rates of the kinetic energy at the borders of the model. Calculated bonding energies and forces strongly depend on surface termination, native oxides, adsorbates, and process control. Twisted starting configurations, steps or rotational misorientations result in special interface configurations mostly no longer perfectly coordinated. Bonding energy and forces are determined not only by the surface structure but also by surface adsorbates as shown by MD of hydrogen on hydrophobic Si and by water-silanol reactions on silica surfaces describing the hydrophilic termination. The simulations lead to a better understanding of the physical processes at the interfaces and support the experimental investigations, especially the electron microscope structure analysis. Simulations based on potentials derived from the bond order expansion are used to enhance the physical reliability of the investigations and to predict the bonding behaviour of a wide variety of semiconductor surfaces.

REFERENCES

1. Q.-Y. Tong and U. Gösele, Semiconductor wafer bonding: Science and technology. Wiley, New York 1999.
2. A. Plößl and G. Kräuter, *Mater. Sci. Eng.* **R25** , 1 (1999).
3. C.M. Goringe, D.R. Bowler, and E. Hernandez, *Rep. Prog. Phys.* **60**, 1447 (1997).
4. D. Conrad and K. Scheerschmidt, *Phys. Rev.* **B58,** 4538 (1998).
5. D. G. Pettifor and I.I. Oleinik, *Phys. Rev.* **B59,** 8487 (1999).
6. D. Conrad, K. Scheerschmidt, and U. Gösele, *Appl. Phys.* **A62**, 7 (1996).
7. D. Conrad, K. Scheerschmidt, and U. Gösele, *Appl. Phys. Lett.* **71**, 2307 (1997).
8. A.Y. Belov, D. Conrad, K. Scheerschmidt, and U. Gösele, *Philos. Magazine* **A77,** 55 (1998).
9. A.Y. Belov, K. Scheerschmidt, and U. Gösele, *phys. status solidi* **171**, 159 (1999).
10. A.Y. Belov, R. Scholz, and K. Scheerschmidt, *Philos. Mag. Lett.* **79**, 531 (1999).
11. C. Koitzsch, D. Conrad, K. Scheerschmidt, and U. Gösele, *J. Appl. Phys.* **88**, 7104 (2000).
12. J. Tersoff, *Phys. Rev.* **B38**, 9902 and **B39**, 5566 (1989).
13. D. Conrad, K. Scheerschmidt, and U. Gösele, *Appl. Phys. Lett.* **71**, 49 (2000).
14. S. H. Garofalini, *Electrochem. Soc. Proc.* **93-29,** 57 (1994).
15. D. Timpel, M. Schaible, K. Scheerschmidt, *Journ. Appl. Phys.* **85,** 2627 (1999).
16. K. Scheerschmidt, D. Conrad, A. Belov, H. Stenzel, *Electrochem. Soc. Proc.* **97-36**, 381 (1998).
17. F.H. Stillinger and T.A. Weber, *Phys. Rev.* **B31**, 5262 (1985).
18. S. H. Garofalini, *J. Non-Cryst. Solids* **120**, 1 (1990).
19. A.J. Dyson and P.V. Smith, *Surface Science* **355**, 140 (1996).
20. S. Balamane, T. Halicioglu, W.A. Tiller, *Phys. Rev.* **B46,** 2250 (1992).
21. M.I. Baskes, *Phys. Rev.* **B46**, 2727 (1992).
22. J. F. Justo, M.Z. Bazant, E. Kaxiras, V.V. Bulatov, S. Yip, *Phys. Rev.* **B58,** 2539 (1998).
23. Y. C. Wang, K. Scheerschmidt, and U. Gösele, *Phys. Rev.* B **61**, 12864 (2000).
24. J.C. Slater and G.F. Koster, *Phys. Rev.* **94**, 1498 (1954).
25. D.G. Pettifor, *Phys. Rev.* **B63,** 2480 (1989).
26. J.L. Rouviere, K. Rousseau, F. Fournel, and H. Moriceau, *Appl. Phys. Lett.* **77**, 1135 (2000).